

# Pool Boiling Fouling and Corrosion Properties on Liquid-Phase-Deposition TiO<sub>2</sub> Coatings with Copper Substrate

L. L. Wang

Dept. of Chemical Engineering, School of Chemical Engineering and Technology, Tianjin University, Tianjin 300072, China

M. Y. Liu

Dept. of Chemical Engineering, School of Chemical Engineering and Technology, Tianjin University, Tianjin 300072, China

State Key Laboratory of Chemical Engineering, Tianjin 300072, China

DOI 10.1002/aic.12405

Published online September 24, 2010 in Wiley Online Library (wileyonlinelibrary.com).

*Fouling on the heat transfer surfaces of industrial heat exchangers is an intractable problem, and several techniques have been suggested to inhibit fouling. Surface coatings are of such techniques by which the adhesion force between fouling and heat transfer surface can be reduced with low surface free energy thin films. In this article, liquid phase deposition was applied to coat titanium dioxide thin films on the red copper substrates with film thickness in micro- or nano-meter scale. Coating thickness, contact angle, roughness, surface topography, and components were measured with X-ray diffraction, contact angle analyzer, stylus roughmeter, scanning electron microscopy, and energy dispersive X-ray spectroscopy, respectively. Surface free energy of coating layers was calculated based on the contact angle. Heat transfer and fouling characteristics in pool boiling of distilled water and calcium carbonate solution on coated surfaces were investigated. Heat transfer enhancement was observed on coated surfaces compared with untreated or polished surfaces due to the micro- and nano-structured surfaces which may increase the number of nucleation sites. The nonfouling time on the coated surfaces is extended than that on the untreated or polished surfaces due to the reducing of the surface free energy of coated surfaces. Corrosion behavior of coated surfaces soaked in the corrosive media of hydrochloric acid, sodium hydroxide alkali, and sodium chloride salt solutions with high concentration at room temperature a few hours was also explored qualitatively. Anticorrosion results of the coated surfaces were obtained. The coatings resisted alkali corrosion within  $7.2 \times 10^5$  s, acidic corrosion within  $3.6 \times 10^5$  s and salt corrosion within  $2.16 \times 10^6$  s. The present work may open a new coating route to avoid fouling deposition and corrosion on the heat transfer surfaces of industry evaporators, which is very important for energy saving in the related industries.*

© 2010 American Institute of Chemical Engineers *AIChE J.*, 57: 1710–1718, 2011

**Keywords:** liquid phase deposition, coating, fouling, corrosion, pool boiling, TiO<sub>2</sub>

## Introduction

Fouling accumulation on the heat transfer surfaces in the heat exchangers, especially on the surfaces of industry evaporators, is a troublesome problem because it can lead to a

Correspondence concerning this article should be addressed to M. Y. Liu at myliu@tju.edu.cn.

drastic increase of heat resistance and therefore result in a decreased heat-transfer efficiency of heat exchangers.<sup>1-9</sup>

Several approaches toward reduction of fouling adhesion or occurrence on heat transfer surfaces have been suggested in the past years. The most potential techniques are the surface engineering methods which can lower the surface free energy. The reason is that on a surface with high surface free energy, excess adsorption force exists and foulant is easy to adhere on it.<sup>3,6,7,10</sup>

There are generally four types of surface engineering routes.<sup>6</sup> First one is named surface coating characterized with a certain thickness of film layer on the surface to be modified. Surface coating methods include electroplating, chemical plating, physical vapor deposition (sputtering, vacuum evaporation, etc.), chemical vapor deposition, and sol-gel. Second one is called surface modification by which only chemical compositions of the surfaces are changed, and there is no obvious thickness of film layer on the surfaces, such as ion implantation. The third one is called surface treatment by which the texture structure and stress of the surfaces are altered without additional film layer and variation of chemical compositions, such as blasting shot and quenching. The fourth one is the combination of the above three types. Sometimes, all of them are called surface modification.<sup>11</sup>

The most recent crucial work about fouling inhibition on the heat transfer surfaces of the heat exchangers by surface engineering techniques was done by Müller-Steinhagen and coworkers.<sup>11-14</sup> The modified surfaces were characterized with different surface analysis instruments. Fouling experimental results in convective, pool or flow boiling system with typical fouling solutions including simulated milk ultrafiltrate demonstrate that low-energy surfaces, such as the surface with Ni-P-PTFE material layer can significantly reduce the fouling deposition compared with the untreated or polished surfaces.

In spite of these great efforts, a desired surface engineering technique that can meet the demands of industry applications such as process simple, inexpensive, and easy to scale-up still lacks. A surface coating technique called liquid phase deposition (LPD) may be such a method. It was first introduced into the antifouling investigations by Liu et al.<sup>7</sup> Fouling inhibition and flow boiling enhancement on titanium dioxide (TiO<sub>2</sub>) film surfaces coated by LPD on inner wall of heating tube under flow boiling of calcium carbonate (CaCO<sub>3</sub>) solution were observed. TiO<sub>2</sub> being chosen as a coating material is due to its unique characters and potential applications in the energy conservation.

TiO<sub>2</sub>-coated surfaces exhibit super-hydrophilicity when exposing it to an ultraviolet ray. TiO<sub>2</sub> coatings with film thickness in micrometer scale prepared by dipping, sputtering, or plasma-irradiating process can enhance pool boiling, immersion cooling, falling film evaporation, and single water drop evaporation under radiation of ultraviolet ray.<sup>15,16</sup> However, on a super-hydrophobic surface coated with fine particles of nickel and PTFE by means of electrolytic plating with contact angle to water of 152° in room temperature and thickness of  $10 \times 10^{-6}$  m, a stable film boiling occurs in very small superheating, and there is no nucleate boiling region. And the vapor bubbles generated on the surface coalesce into a vapor film without departing from the surface.<sup>17</sup> Hence, the super-hydrophobic Ni-PTFE-coated surface seems

not to be in favor of pool boiling heat transfer. On the other hand, the main reasons resulted in the self-cleaning functions of natural bio-surfaces such as lotus leaves, rice leaves, cicada wings, and water strider legs were contributed to their super-hydrophobic natures and the micro- and nano-scale structures.<sup>18</sup> Therefore, the surface with middle hydrophobicity may be favorable both for boiling enhancement and fouling prevention.

Meanwhile, it is an interesting topic to investigate the fouling behavior on the coated surface with film thickness in micro- or nano-meter scale. The elementary results indicate that antifouling and flow boiling enhancement on TiO<sub>2</sub>-coated surfaces may be improved further if the film thickness of TiO<sub>2</sub> coating layer is near the nanometer scale.<sup>7</sup> To explore the influence of coating layer thickness in a nanometer scale on fouling and heat transfer properties, the coating method of vacuum evaporation was used to prepare TiO<sub>2</sub> film layers, and fouling deposition in pool boiling of CaCO<sub>3</sub> solution was investigated.<sup>19</sup> The results indicate that all TiO<sub>2</sub> coating surfaces can inhibit CaCO<sub>3</sub> deposition, and the fouling induction time on TiO<sub>2</sub> coating surface in pool boiling with film thickness of  $8 \times 10^{-8}$  m is about 50 times longer than that of untreated or polished surface. However, the vacuum evaporation coating method is more expensive and more difficult to scale up compared with the LPD method which is more attractive for industry applications.

Anticorrosion investigations on these coated surfaces are also meaningful because sometimes heat transfer fluids are the corrosive media. Shen et al.<sup>20</sup> investigated the corrosion resistance characteristics of TiO<sub>2</sub> nanoparticle coating with film thickness of from  $1.96 \times 10^{-7}$  m to  $6.40 \times 10^{-7}$  m on 316 L stainless steel substrate by a sol-gel method and found that the sample with thickness of  $4.64 \times 10^{-7}$  m has an excellent anticorrosion behavior in the NaCl solution with concentration of less than  $1000 \text{ M m}^{-3}$  and pH higher than 2. With high concentration or acidic solution environment, the TiO<sub>2</sub> films will dissolve gradually and the anticorrosion ability of the TiO<sub>2</sub> films decrease greatly. It is known that film characters are very sensitive to the preparation process. The substrate and its surface state also influence the features of the films. However, no work is available in the literature on the anticorrosion function of TiO<sub>2</sub> coatings prepared by LPD on the copper substrates with strong acid, alkali, and salt solutions at high concentrations.

The goal of this work is to study the fouling as well as the corrosion characteristics of TiO<sub>2</sub>-coated surfaces prepared by LPD in the micro- and nano-meter scale. The first part of this article presents the experimental description including the preparation, characterization of test surfaces, pool boiling, and corrosion experiments on test samples. The second part contains the experimental results and discussion. The last part is the concluding remarks.

## Experimental

### *Preparation and characterization of TiO<sub>2</sub>-coated surfaces*

*Preparation of TiO<sub>2</sub>-Coated Surfaces by LPD.* The test substrates used in the present experiments are red copper plates. The size of test substrates for characterization is

about  $0.01 \times 0.01 \times 0.007 \text{ m}^3$  and that for heat transfer and fouling experiments is 0.1 m in diameter and 0.007 m in thickness. Three types of test surfaces were prepared: untreated, polished, and coated surfaces.

Polished test samples were prepared from untreated substrates by finishing, polishing, oil removing, cleaning, and drying. Finishing was carried out by using emery wheel with emery grits of Nos. 340 and 600. Polishing was performed by using polishing wheel with grinding pastes of emery sand particles in diameter of  $1 \times 10^{-6}$  and  $0.5 \times 10^{-6} \text{ m}$ . Deoiling was done by using 10% sodium hydroxide solution. Cleaning includes acetone ultrasonic cleaning and deionized water cleaning. Airing was carried out with natural air.

TiO<sub>2</sub> thin layers were coated on polished surfaces with LPD method. The polished samples after being dried were dipped into the homogeneous reaction solution in a reactor with a temperature control device. Deposition reactions began at proper reaction conditions, including concentrations of chemicals, temperature, reaction time, etc. Test samples were treated in an electric muffle furnace (Type DRZ-4) including cleaning, drying, and heat treating after deposition reaction finished. The temperature of heat treatment increased at a rate of 2 K per 60 s and then was kept in 423.15 K for 3600 s.

*Characterization of TiO<sub>2</sub>-Coated Surfaces.* The surface topography of test samples was measured with SEM (Philips, XL-30 type). The root mean square roughness Ra was measured with JB-8C type surface stylus roughmeter with a resolution of  $1 \times 10^{-9} \text{ m}$ .

The coating thickness of the samples was determined by using wide-angle X-ray diffraction (XRD). XRD measurement was performed with X-ray diffractometer (Rigaku D/MAX 2200V/PC type). The average film thickness was calculated based on the diffraction integrated intensity of substrate material copper (Cu).

The contact angles were measured by using both digital camera and JY-82 contact angle analyzer under room temperature. Distilled water and glycerin were used as test liquids. The contact angle on each test sample was measured at three times, and the average was taken as the measured result. The average relative error percentage of the contact angle measurement values between the two methods is less than 8%.

The surface free energy was calculated on the measurement data of contact angles of coating surfaces according to GEOs method.<sup>21</sup>

The amorphous TiO<sub>2</sub> coatings were characterized by SEM and energy dispersive X-ray spectroscopy (EDX) (Oxford ISIS300 type).

### Experiments of pool boiling and fouling

The pool boiling experimental apparatus, flowchart, parameter measurements and calculations, fluid media, and operation conditions are available in literature and only described here briefly.<sup>19</sup>

The experimental apparatus consists of a cylindrical stainless steel tank with inner diameter of 0.1 m and height of 0.3 m, a cylindrical copper heater with diameter of 0.08 m and height of 0.06 m wrapped with heating resistance wire and a glass condenser with heat-transfer area of 0.02 m<sup>2</sup>.

The temperature measuring system consists of a few Pt resistance transducers, a signal amplifier, an A/D converter, and an industrial computer 610. The temperatures along the center axis of the copper cylinder heater were measured by three Pt resistances embedded in the cylinder. Liquid temperature in boiling pool was also measured by Pt resistance.

Pool boiling of distilled water and CaCO<sub>3</sub> solution on different test surfaces was carried out. The operation was continuous for each test surface. The experiments were performed at atmospheric pressure. The data were recorded in an interval of 1800 s. In each time for data recording, the data were sampled with a frequency of 10 Hz and time length of 10 s. Heat flux and boiling surface temperature were determined by using three temperatures in the cylindrical heater and their axial locations according to one-dimensional conduction theory. The heat resistance of coating layer is ignored during the surface temperature calculation because the coating thickness is in a micro- or nano-meter scale. Heat transfer coefficient of pool boiling was calculated based on the heat flux and heat-transfer temperature difference.

CaCO<sub>3</sub> water solution was prepared by dissolving a certain amount of analytical grade CaCl<sub>2</sub> ( $0.0721 \text{ kg m}^{-3}$ ) and NaHCO<sub>3</sub> ( $0.1092 \text{ kg m}^{-3}$ ) in distilled water with temperature of 293 K. The concentration of the saturated CaCO<sub>3</sub> water solution was  $65 \times 10^{-3} \text{ kg m}^{-3}$ . The control of the solution chemistry is enough to obtain good experimental results.

### Experiments on corrosion resistance

The corrosion behavior of TiO<sub>2</sub> coatings in the corrosive media (strong acid, alkali, and salt solutions) with high concentration was investigated qualitatively to test the ability to resist corrosion of heat transfer media. During the corrosion resistance experiments, the test samples were immersed in the corrosive media a certain time at room temperature. The corrosive media included sodium chloride, hydrochloric acid, and sodium hydroxide solutions with the concentrations of 25, 30, and 30%, respectively. After a few hours, the test sample was taken out from the solution to observe its corrosion property.

## Results and Discussion

### Characterization of TiO<sub>2</sub>-coated surfaces

*SEM.* Typical SEM images of test samples are presented in Figure 1. It can be seen that the surface microstructure of untreated sample is quite rough. While, polished and coated surfaces (Figures 1b, c) are smooth. Hence, LPD process does not change the surface morphology of test sample too much.

*Coating Thickness.* Figure 2 illustrates typical XRD patterns of test samples and SEM/EDX plots of a similar sample. Figure 2b is the enlarged views of the highest diffraction peaks in the XRD curves.

In Figure 2a, there are three obvious spikes showing the existence of substrate material of Cu, and one of them is the highest indicating the largest diffraction intensity of substrate material of Cu. The largest value of diffraction intensity at double diffraction angle for each sample is listed in Table 1.



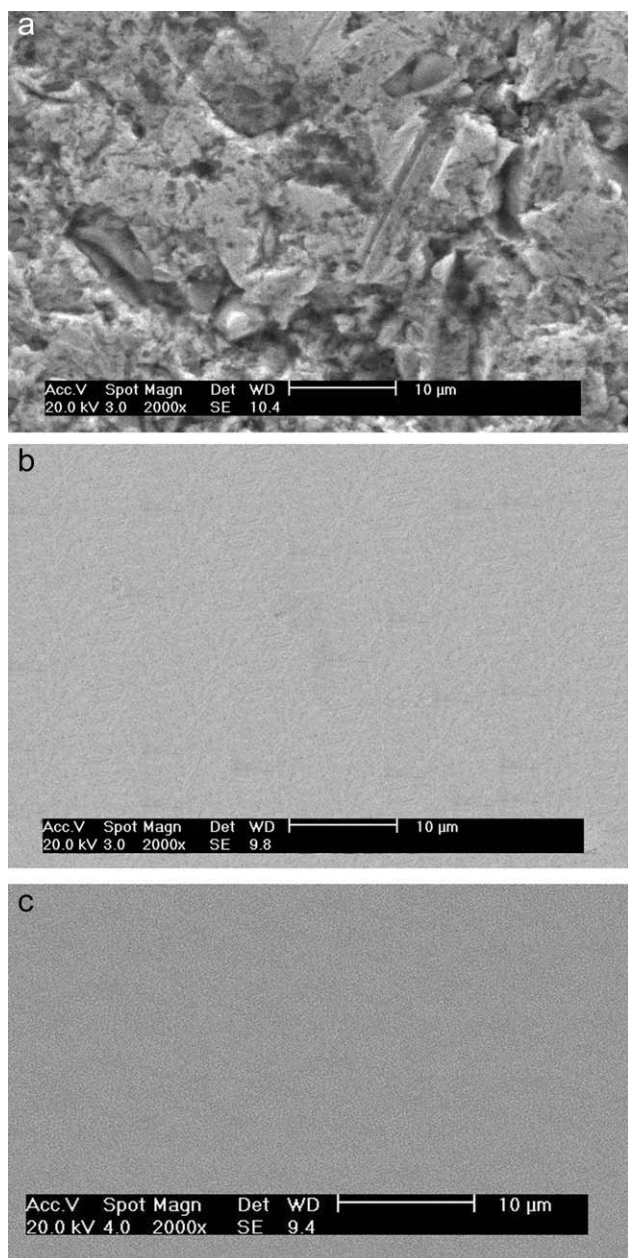


**Figure 1. SEM images of test surfaces.**

(a) Untreated surface; (b) polished surface; (c) coated surface,  $\delta = 8.35 \times 10^{-7}$  m.

It is found from Table 1 and Figure 2b that the largest value of diffraction intensity at double diffraction angle of about  $43.29^\circ$  decreases gradually with the increase of the coating thickness. In other words, the highest diffraction peak of polished substrate is the highest and that of the coated substrate reduces due to the absorption of ray energy. With the increase of film thickness, the absorption amount of ray energy of coated film increases, leading to the decrease in height of highest diffraction peak. It is by this difference that the coating thickness of coated samples is estimated. The thicknesses of the four  $\text{TiO}_2$  films measured were  $4.58 \times 10^{-7}$ ,  $7.44 \times 10^{-7}$ ,  $8.35 \times 10^{-7}$ , and  $15.59 \times 10^{-7}$  m, respectively.

There are three crystalline phases or crystalline forms for the crystal  $\text{TiO}_2$ . They are anatase phase and brookite phase at low temperature and rutile phase at high temperature, which can be detected by the instruments of XRD. Generally, the characteristic peak of anatase phase  $\text{TiO}_2$  appears at the double diffraction angle of about  $25^\circ$ . However, on the XRD curves of coated substrates (see Figure 2a) only very weak spikes are observed at the double diffraction angle of about  $24^\circ$  which may show the noise. The main reason for this phenomenon is that the heat treating temperature of the coated samples is low and no enough  $\text{TiO}_2$  crystals are formed and the  $\text{TiO}_2$  coating structure is amorphous. Figure 2c gives a typical EDX plot coupled with SEM plot of a similar sample to analyze the surface chemistry compositions. The substrate was not well polished, but this does not affect the chemistry composition analysis results. It can be seen from Figure 2c that the mass percentage of Ti (wt %) on the sample surface is 3.10%, and the atom percentages (at %) 3.32%. EDX and SEM analyses indicate that the LPD coating is composed of O, Ti, and Cu elements.

The profiles of the peaks are similar both for the sample of copper substrate and the coated ones. The shoulder peaks in the enlarged XRD curves in Figure 2b result from the  $K_{\alpha 2}$ . The shift of the peak in Figure 2b is random, and the shift double diffraction angles are small, ranging from  $0.01$  to  $0.05^\circ$ . The shift is caused by the possible position deviations of the test samples during XRD measurements.

**Surface Roughness.** The value of root mean square roughness for untreated surface is about  $3.72 \times 10^{-7}$  m. For polished surface,  $R_a$  is about  $0.83 \times 10^{-7}$  m. For coated surfaces,  $R_a$  varies from  $0.31 \times 10^{-7}$  to  $0.54 \times 10^{-7}$  m.

**Contact Angle.** Table 2 shows the measured data of contact angles. The contact angle increases sharply when the surfaces are coated with  $\text{TiO}_2$  film layers except when the coating thickness is  $15.59 \times 10^{-7}$  m. No great variations of contact angles can be observed when the coating layer thickness climbing. The contact angle of glycerin is near the same as that of the distilled water.

**Surface Free Energy.** The physical meaning of surface free energy is necessary work done by overcoming the attractive force between two surfaces, and the calculated values of surface free energy are also shown in Table 2. Figure 3 illustrates the relationship between surface free energy and the coating thickness. The values of coating thickness for the untreated and polished samples are both zero. But to draw the two bars in the same chart for comparison, we let the thickness value for the untreated sample to be  $-2 \times 10^{-7}$  m in Figure 3.

It can be found that surface free energy of  $\text{TiO}_2$  coatings decreases obviously compared with those of untreated and polished surfaces, and it increases steeply again when the coating thickness exceeds  $15.59 \times 10^{-7}$  m.

### ***Influence of surface modification on heat transfer of pool boiling of distilled water***

To verify the reproducibility of the data, repeated experiments of pool boiling with distilled water were done on the untreated copper substrate under heat flux of 79.8, 96.6, and  $110 \text{ kW m}^{-2}$ . The time interval of the two experiments is 2 weeks. The results are shown in Figure 4. It can be said that experimental reproducibility is good.

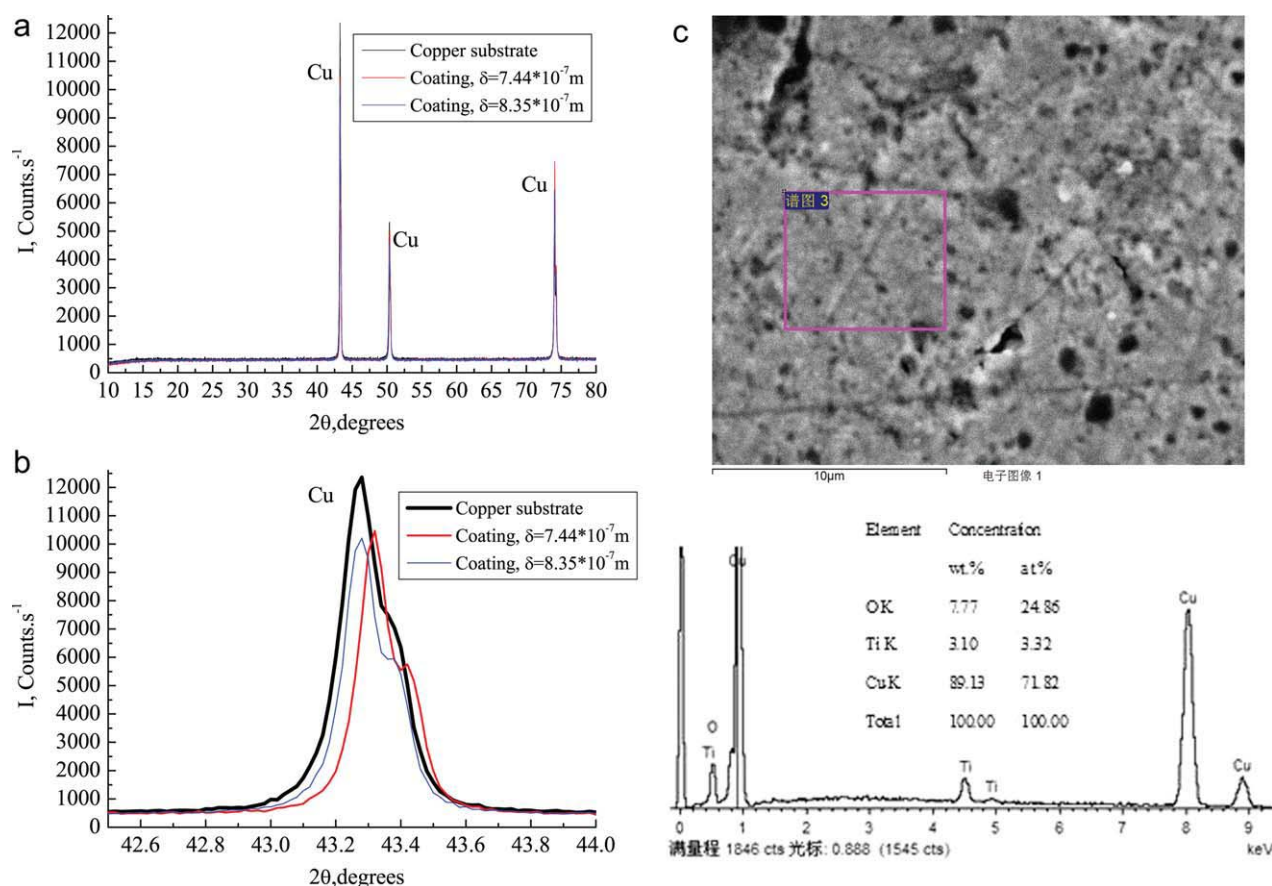


**Figure 2. Typical XRD patterns of test samples and SEM/EDX plots.**

(a) XRD plots; (b) highest diffraction peaks in the XRD plots; (c) SEM/EDX plots [Color figure can be viewed in the online issue, which is available at [wileyonlinelibrary.com](http://wileyonlinelibrary.com)].

The relationship between the pool boiling heat transfer coefficient on the test surfaces and operation time when heat flux is  $96.6 \text{ kW m}^{-2}$  is presented in Figure 5.

Comparing with the data on untreated sample, the heat-transfer coefficients on polished surface are slightly higher, as shown in Figure 5. But they are all less than that on  $\text{TiO}_2$ -coated surfaces, indicating that pool boiling of distilled water is enhanced due to the appearance of  $\text{TiO}_2$  coating layer on the copper substrates. However, the relationship between the coating thickness and the boiling coefficient is not obvious. The coefficients on coated surface with thickness of  $8.35 \times 10^{-7} \text{ m}$  are the largest, following by those on coated surfaces with thickness of  $7.44 \times 10^{-7}$  and  $15.59 \times 10^{-7} \text{ m}$ . The reason may be that the coating thickness is too thin. Meanwhile, the heat transfer coefficients on the coated surfaces with thickness of  $7.44 \times 10^{-7}$  and  $8.35 \times 10^{-7} \text{ m}$  are quite different even though they are almost equal in the surface free energy (about  $20 \text{ mJ m}^{-2}$ ). This may mean that pool boiling is not only affected by the contact angle and surface free energy or the surface material (since surface free energy depends largely on the inherent property of coating material itself) but also is influenced by the other factors such as the surface microstructure characteristics.

The work of Takata et al.<sup>15,16</sup> focused on the effect of surface wettability (changing the hydrophilicity of  $\text{TiO}_2$  surface by ultraviolet irradiation) on the maximum heat flux in the

pool boiling heat transfer. Their data showed that maximum heat flux of  $\text{TiO}_2$ -coated surfaces is higher than that of non-coated due to the increase of surface wettability resulted from the photo-induced superhydrophilicity. Referencing to the nucleate boiling,<sup>15,16</sup>  $\text{TiO}_2$ -sputtered surface with thickness of  $2.5 \times 10^{-7} \text{ m}$  has higher nucleate boiling heat transfer coefficients compared with other samples, but  $\text{TiO}_2$ -dipped sample  $4 \times 10^{-6} \text{ m}$  has worse heat transfer characteristics than the noncoated ones, and they felt this difference was due to the different thermal conductivity of the coating materials.

Investigations on the pool or flow boiling of nanofluids or pure water on plain surfaces or porous coating surfaces indicate that the surface modification due to the buildup of a porous layer of nanoparticles on the heated surface during boiling, which can improve surface wettability and promote liquid rewetting is the principal mechanism by which maximum heat flux is enhanced with nanofluids.<sup>22–26</sup> For the

**Table 1. The Largest Values of Diffraction Intensity at Double Diffraction Angle for Three Test Samples**

Polished Surface		Coated Surface, $\delta = 7.44 \times 10^{-7} \text{ m}$		Coated Surface, $\delta = 8.35 \times 10^{-7} \text{ m}$	
$2\theta, ^\circ$	I, Counts·s <sup>-1</sup>	$2\theta, ^\circ$	I, Counts·s <sup>-1</sup>	$2\theta, ^\circ$	I, Counts·s <sup>-1</sup>
43.29	11,840	43.34	10,009	43.30	9729

**Table 2. Measurement Results of Contact Angle and Surface Free Energy of Test Samples**

Test Samples of Different Surfaces	Contact Angle of Distilled Water, $\theta_w/^\circ$	Contact Angle of Glycerin, $\theta_g/^\circ$	Surface Free Energy, $\gamma/\text{mJ m}^{-2}$
Untreated	73.13	79.81	37.85
Polished	75.75	82.83	36.39
Coated, $\delta = 4.58 \times 10^{-7} \text{ m}$	93.50	92.67	16.16
Coated, $\delta = 7.44 \times 10^{-7} \text{ m}$	93.25	93.80	16.74
Coated, $\delta = 8.35 \times 10^{-7} \text{ m}$	93.25	96.83	18.85
Coated, $\delta = 15.59 \times 10^{-7} \text{ m}$	80.75	84.28	27.66

nucleate boiling, however, the nanofluid has poor heat transfer performance compared to pure water because the nanoparticles reduce the number of active nucleation sites with variation of surface roughness even though the maximum heat flux is enhanced.<sup>22</sup>

Hence, the nucleate boiling process is complex, and the heat transfer coefficients of coated surfaces are affected by surface preparation methods, coating material conductivity, coating layer thickness, inner pore structure, etc. The mechanism explanations of heat transfer enhancement are also not well determined.

The work of Takata et al.<sup>15,16</sup> indicates that thin coatings improve nucleate boiling and thick coatings deteriorate it. In our work, the thickness of most coatings is too thin compared with that reported by Takata et al. Hence, only heat transfer enhancement was obtained. The increase of boiling heat transfer coefficient on the surfaces of  $\text{TiO}_2$  coating is considered to be due to the micro- and nano-meter coating surfaces. Compared with untreated and polished surfaces, the surfaces of LPD coatings are not as solid as those of the substrates but as close as those of the macro- and micro-meter coatings. For the nucleate boiling heat transfer, these coatings may increase the number of active nucleation sites, reducing the nucleate boiling superheat.

Generally, in the nucleate boiling region, at given temperature difference between the solution and the heat transfer surface, more active nucleation sites (here referring to the small vapor bubbles, not the crystal growth) mean larger number of

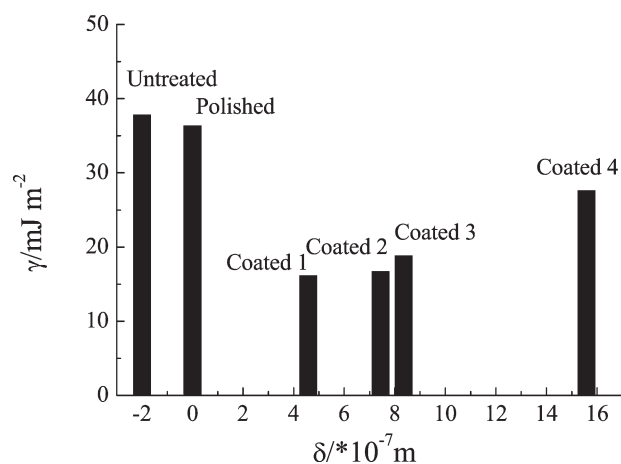


**Figure 3. Surface free energy of test samples vs. coating layer thickness.**

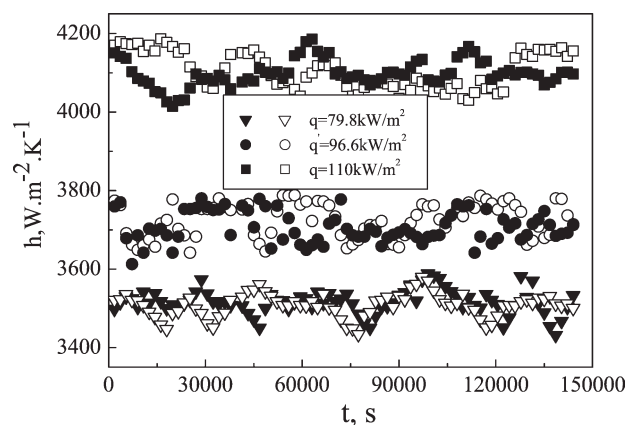


**Figure 4. Repeated experiments of distilled water in pool boiling on untreated copper substrate.**

small vapor bubbles at given time or higher frequency of small vapor bubbles and thinner heat transfer boundary layer thickness due to the stirring of the vapor bubbles. Thus, higher boiling heat transfer rate or boiling coefficients can be obtained. On the other hand, smaller number of nucleation sites means smaller number of vapor bubbles at given time or lower frequency of vapor bubbles and thicker heat transfer boundary layer thickness. Extremely, if no nucleation sites are formed on the heat transfer surface, the boiling heat transfer rate or the boiling coefficient is zero.

#### ***Influence of surface modification on fouling in pool boiling of $\text{CaCO}_3$ solution***

Typical fouling experimental results with heat flux of  $96.6 \text{ kW m}^{-2}$  are exhibited in Figure 6. As shown in Figure 6, the heat transfer enhancement is obvious at the beginning of running time on the  $\text{TiO}_2$ -coated surfaces, and the increase trendly with the coating thickness is the same as that of the distilled water. After a relatively long period of time, the coefficient declines sharply due to the deposition of  $\text{CaCO}_3$  fouling on the test surfaces and finally reaches a much lower coefficient value. The time when the heat transfer coefficient starts to decline (corresponding to end of the fouling induction time in the curve of heat resistance vs. time that does

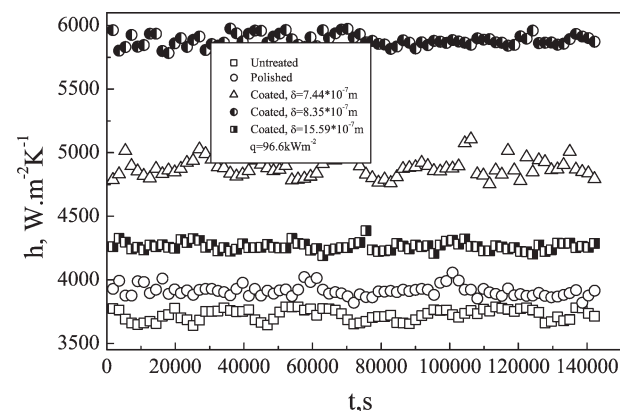


**Figure 5. Pool boiling heat-transfer coefficients on the test surfaces vs. running time.**



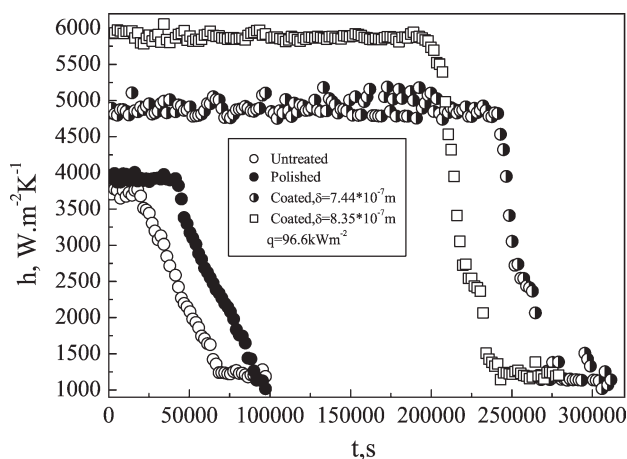


**Figure 6. Heat transfer coefficients vs. operation time on different test surfaces in pool boiling of  $\text{CaCO}_3$  solution.**

not show here) is different for distinct test surfaces which may result from the variation of surface parameters, such as the surface free energy. Under the present conditions, the periods of without fouling deposition for the untreated surface, polished surface, and coated surfaces with thickness of  $7.44 \times 10^{-7}$  and  $8.35 \times 10^{-7}$  m are about  $2.4 \times 10^4$ ,  $4.2 \times 10^4$ ,  $2.4 \times 10^5$ , and  $2.1 \times 10^5$  s, respectively. Hence, the  $\text{TiO}_2$ -coated surfaces are much better than the untreated or polished as the coated surfaces can run without fouling in a much longer time even though the reduction speed of boiling heat transfer coefficient of coated surfaces is slightly higher than that of the non-coated surfaces after the fouling begins to form.

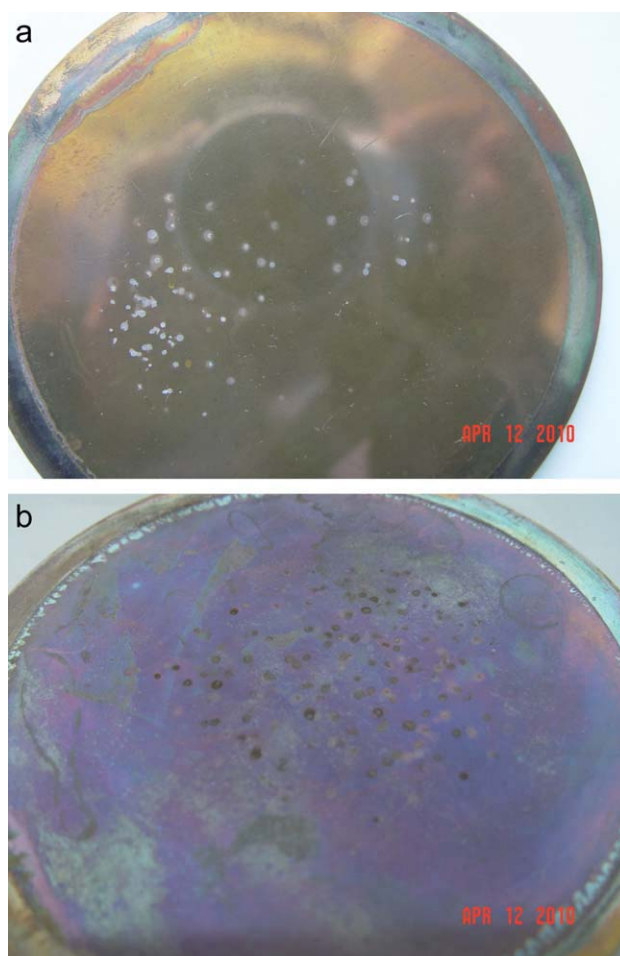
A surface with high surface free energy tends to absorb certain dirt to reduce its additional surface free energy. With time running, the thickness of fouling layer climbs, and heat resistance also increases, leading to a reduction of heat transfer coefficient and ultimately reaching to a stable low value. On the surface with lower surface free energy, fouling is more difficult to deposit, and fouling induction period is enlarged.

Figure 7 shows the digital photos of the coated surfaces after the fouling experiments. Generally, a yellow surface (Figure 7a) indicates there is a thinner  $\text{TiO}_2$  coating layer on the substrate and a purple one (Figure 7b) means a thicker  $\text{TiO}_2$  film. It can be seen that there are several white  $\text{CaCO}_3$  fouling spots with diameter of 0.001–0.002 m on both coated copper plates. The fouling is more serious on the thicker surface after the fouling experiments were finished since there are about 100 spots on it. While on the thinner one, there are about 70 spots on it. The value of root mean square roughness for the thinner coated surface is  $0.54 \times 10^{-7}$  m and for the thicker one is  $0.42 \times 10^{-7}$  m.

The fouling induction period refers to the time length starting from the contact between the clean surface in heat exchanger and the solution to the time when the deposit was able to be detected.<sup>4</sup> This period may last anytime from few seconds to several days. Before the induction time, the initially high heat transfer coefficients remain unchanged. During this time, a few nuclei for crystallization are formed and scattered on the heat transfer surface. Generally, no induction period occurs for particulate fouling. If the measuring method is enough sensitive, fouling on

surfaces under pool boiling should not show induction period. However, the induction time is influenced by many factors such as concentrations of solutions, fouling types, states of heat transfer surfaces, surface temperature, measuring accuracy of sensor, etc. For super-saturation solution of  $\text{CaCO}_3$  in pool boiling, the rates of nucleation and growth of crystallization are not infinite. Hence, a fouling induction period can occur on the untreated surfaces for the pool boiling system,<sup>27</sup> as shown in Figure 6.

For pool boiling of water, the values of heat transfer coefficients in this work are lower than those reported in the literature. There maybe several reasons for this. One relates to the system error of experimental apparatus. There are so many factors that affect the final results of coefficients, such as the geometry shape of boiling surface or sample (such as tube and plate), water pool size and shape, operation and environment conditions, measurement methods of parameters of temperature, and heat flux. For different authors, the difference in magnitude of heat transfer coefficient of pool boiling can reach 20 times. Another one may relate to the neglect of heat conductivity of coating material on the heat transfer surface. The third one may be the error of heat flux calculation.



**Figure 7. Digital photos of coated surfaces after the fouling experiments with heat flux  $q$  of  $96.6 \text{ kW m}^{-2}$ .**

(a)  $\delta = 7.44 \times 10^{-7}$  m; (b)  $\delta = 8.35 \times 10^{-7}$  m [Color figure can be viewed in the online issue, which is available at [wileyonlinelibrary.com](http://www.wileyonlinelibrary.com)].

**Table 3. Results of Corrosion Resistance Experiments**

Corrosive Media	Immersion Time (s)	Description of Experimental Results	
		Untreated Surface	Coated Surface
25% NaCl solution	$2.16 \times 10^6$	Slight corrosion (Fig. 8b <sub>2</sub> ).	No corrosion after $7.2 \times 10^5$ s and coated film was eroded and original surface of substrate was observed until after $2.16 \times 10^6$ s (Fig. 8b <sub>1</sub> ).
30% HCl solution	$3.6 \times 10^5$	Serious corrosion with dark surface (Fig. 8c <sub>2</sub> ).	Serious corrosion with dark surface (Fig. 8c <sub>1</sub> ).
30% NaOH solution	$7.2 \times 10^5$	Serious pit corrosion (Fig. 8d <sub>2</sub> ).	No coating breakage was found for coated surface, and serious pit corrosion was seen on uncoated surface (Fig. 8d <sub>1</sub> ).

Fortunately, the relative values of boiling coefficients and the comparison results between different surfaces are more important. Keeping this in mind, the results of heat transfer coefficients are still meaningful. A measure that uses a new type of pool boiling apparatus will be taken to test the issue of datum difference from literature.

#### **Anticorrosion property of coated surfaces**

Experimental results of corrosion resistance on the coated surfaces are shown in Table 3. Digital images of surface topography of samples before and after corrosion experiment are shown in Figure 8.

The experimental results indicate that in acidic solution environment both coated and untreated test samples are easy to be corroded, and the coating layer does not improve the surface character of corrosion resistance. In alkali solution environment, the behavior of corrosion resistance of coated

sample is better than that of untreated sample in the experimental period. In the salt solution, coated film can resist corrosion until  $2.16 \times 10^6$  s.

It is noted that this study is in its early stage. However, the contents are new and are meaningful for the possible industry applications. Of course, much further work is needed to examine the accurate values of coating thickness and pool boiling coefficient on the coatings, to verify the existence of the induction period in pool boiling, to investigate quantitatively the corrosion behavior on these coatings, to obtain well accepted mechanism explanations of nucleate boiling enhancement and antifouling on coating surfaces and to find the optimum parameters of the coatings by designing strictly control, quantitative and visual experiments. In addition, new coating materials that can stand against acidic environment should be found. New surface modification method is also needed to improve the durability of the coatings. These related topics are being considered or carried out at present in our laboratory.

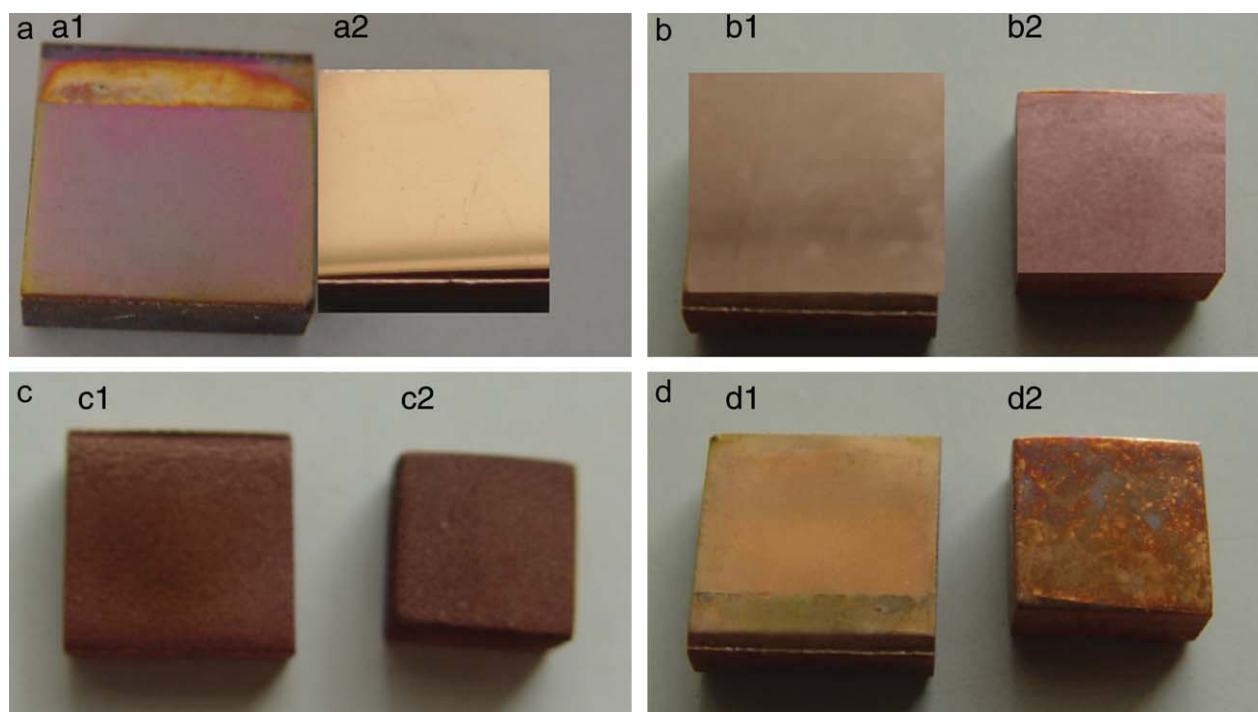


**Figure 8. Digital images of test samples before and after experiments of corrosion resistance.**

(a) Before corrosion experiment; (b) after  $2.16 \times 10^6$  s in 25% NaCl solution; (c) after  $3.6 \times 10^5$  s in 30% HCl solution; (d) after  $7.2 \times 10^5$  s in 30% NaOH solution. 1-Coated; 2-Untreated [Color figure can be viewed in the online issue, which is available at [wileyonlinelibrary.com](http://wileyonlinelibrary.com)].



## Concluding Remarks

LPD was successfully used to coat TiO<sub>2</sub> film layer in micro- or nano-meter scale on the red copper substrate. Pool boiling heat transfer and fouling experiments on these coating surfaces were carried out with distilled water and CaCO<sub>3</sub> solution as work fluids. In addition, the qualitative experiments of corrosion resistance on these surfaces in acid, alkali, and salt solutions with high concentrations were also performed.

Pool boiling is enhanced and fouling induction period is enlarged on the coated surfaces. The key factors that influence pool boiling heat transfer and fouling include the surface coating micro- and nano-meter structure, surface free energy, and coating method. Heat transfer enhancement on the coated surfaces compared with untreated or polished surfaces is due to the micro- and nano-structured surfaces which may increase the number of nucleation sites, and antifouling results from the reducing of the surface free energy. Within the present conditions, coated surface can resist corrosion in certain degree in alkali and salt solution environments. This work may help us to find a new multi-function heat-transfer surface, which is crucial for energy saving in the process industries. One further important topic should focus on detailed investigations on antifouling and heat transfer enhancement mechanisms.

## Acknowledgments

The authors are grateful to the National Natural Science Foundation of China (Grant No.20876106), Natural Science Foundation of Tianjin (Key Program Grant No.09JCZDJC24100), and the Cheung Kong Scholar Program for Innovative Teams of the Ministry of Education of China (Grant No. IRT0641) for the financial support of this work. The authors also thank Profs. S. R. Yang, Z. M. Xu, X. G. Ren, Q. F. Yang for their valuable suggestions and PhD candidate Y. W. Cai and undergraduate B. Zhu for their help during preparation of this manuscript.

## Notation

- $h$  = heat-transfer coefficient in pool boiling, W·(m<sup>2</sup> K)<sup>-1</sup>  
 $I$  = XRD integrated intensity, counts·s<sup>-1</sup>  
 $q$  = heat flux, W m<sup>-2</sup>  
 $t$  = time, s  
 $\gamma$  = surface free energy, J m<sup>-2</sup>  
 $\delta$  = thickness of coating layer, m  
 $\theta_w$  = contact angle of distilled water, °  
 $\theta_g$  = contact angle of glycerin, °  
 $\theta$  = diffraction angle, °

## Subscript

- $g$  = glycerin as test liquid  
 $w$  = distilled water as test liquid

## Literature Cited

- Branch CA, Müller-Steinhagen H. Influence of scaling on the performance of shell-and-tube heat exchangers. *Heat Transf Eng.* 1991;12:37–45.
- Steinhagen R, Müller-Steinhagen H, Maani K. Problems and costs due to heat exchanger fouling in New Zealand industries. *Heat Transf Eng.* 1993;14:19–30.
- Müller-Steinhagen H, Zhao Q. Investigation of low fouling surface alloys made by ion implantation technology. *Chem Eng Sci.* 1997;52:3321–3332.
- Yang SR, Xu ZM, Sun LF. *The Fouling of Heat Exchanger and the Countermove (in Chinese, 2nd edition)*. Beijing: Science Press, 2004.
- Müller-Steinhagen H, Malayeri MR, Watkinson A. Fouling of heat exchangers—new approaches to solve an old problem. *Heat Transf Eng.* 2005;26:1–4.
- Liu MY, Wang H, Wang Y. Progress on antifouling and heat transfer in boiling evaporators with surface engineering methods. *Chem Prog (in Chinese)*. 2007;26:442–447.
- Liu MY, Wang H, Wang Y. Enhancing flow boiling and antifouling with nanometer titanium dioxide coating surfaces. *AIChE J.* 2007;53:1075–1085.
- Herz A, Malayeri MR, Müller-Steinhagen H. Fouling of roughened stainless steel surfaces during convective heat transfer to aqueous solutions. *Energy Convers Manage.* 2008;49:3381–3386.
- Bansal B, Chen XD, Müller-Steinhagen H. Analysis of “classical” deposition rate law for crystallisation fouling. *Chem Eng Process.* 2008;47:1201–1210.
- Foerster M, Augustin W, Bohnet M. Influence of the adhesion force crystal/heat exchanger surface on fouling mitigation. *Chem Eng Process.* 1999;38:449–461.
- Santos O, Nylander T, Rosmaninho R, Rizzo G, Yiantsios S, Andritsos N, Karabelas A, Müller-Steinhagen H, Melo LS, Boulangé-Petermann L, Gabet C, Braem A, Trägårdh C, Paulsson M. Modified stainless steel surfaces targeted to reduce fouling-surface characterization. *J Food Eng.* 2004;64:63–79.
- Rosmaninho R, Santos O, Nylander T, Paulsson M, Beuf M, Benezech T, Yiantsios S, Andritsos N, Karabelas A, Rizzo G, Müller-Steinhagen H, Melo LF. Modified stainless steel surfaces targeted to reduce fouling-evaluation of fouling by milk components. *J Food Eng.* 2007;80:1176–1187.
- Rosmaninho R, Melo LF. Protein-calcium phosphate interactions in fouling of modified stainless-steel surfaces by simulated milk. *Int Dairy J.* 2008;18:72–80.
- Rosmaninho R, Rizzo G, Müller-Steinhagen H, Melo LF. Deposition from a milk mineral solution on novel heat transfer surfaces under turbulent flow conditions. *J Food Eng.* 2008;85:29–41.
- Takata Y, Hidaka S, Cao JM. Effect of surface wettability on boiling and evaporation. *Energy.* 2005;30:209–220.
- Takata Y, Hidaka S, Masuda M, Ito T. Pool boiling on a superhydrophilic surface. *Int J Energy Res.* 2003;27:111–119.
- Takata Y, Hidaka S, Uruguchi T. Boiling feature on a super water-repellent surface. *Heat Transf Eng.* 2006;27:25–30.
- Gao XF, Jiang L. Recent studies of natural superhydrophobic bio-surfaces. *Physics.* 2006;35:559–564.
- Wang Y, Liu MY, Wang H. Antifouling and enhancing pool boiling by TiO<sub>2</sub> coating surface in nanometer scale thickness. *AIChE J.* 2007;53:3062–3076.
- Shen GX, Chen YC, Lin CJ. Corrosion protection of 316 L stainless steel by a TiO<sub>2</sub> nanoparticle coating prepared by sol-gel method. *Thin Solid Films.* 2005;489:130–136.
- Michalski MC, Hardy J, Saramago BJV. On the surface energy of PVC/EVA polymer blends comparison of different calculation methods. *J Colloid Interface Sci.* 1998;208:319–328.
- Bang IC, Chang SH. Boiling heat transfer performance and phenomena of Al<sub>2</sub>O<sub>3</sub>–water nano-fluids from a plain surface in a pool. *Int J Heat Mass Transf.* 2005;48:2407–2419.
- Coursey JS, Kim J. Nanofluid boiling: the effect of surface wettability. *Int J Heat Fluid Flow.* 2008;29:1577–1585.
- Jeong YH, Chang WJ, Chang SH. Wettability of heated surfaces under pool boiling using surfactant solutions and nano-fluids. *Int J Heat Mass Transf.* 2008;51:3025–3031.
- Kim HD, Kim J, Kim MH. Experimental studies on CHF characteristics of nano-fluids at pool boiling. *Int J Multiphase Flow.* 2007;33: 691–706.
- Sarwar MS, Jeong YH, Chang SH. Subcooled flow boiling CHF enhancement with porous surface coatings. *Int J Heat Mass Transf.* 2007;50:3649–3657.
- Ren XG, Li CQ, Liu CH, Zhao Q. Surface treatment of heater by dynamic mixing ion implantation for inhibiting calcium sulfate deposition. *Petroleum Process Petrochemicals (in Chinese)*. 2001;32:56–59.

Manuscript received Dec. 5, 2009, and revision received Aug. 3, 2010.